ELSEVIER

Polymer 42 (2001) 3679–3686

polymer

www.elsevier.nl/locate/polymer

Preparation of ultra-high modulus materials from metallocene based linear polyethylenes

M. Al-Hussein, G.R. Davies, I.M. Ward*

IRC in Polymer Science and Technology, Department of Physics and Astronomy, University of Leeds, Woodhouse Lane, Leeds LS2 9JT, UK

Received 26 June 2000; accepted 1 August 2000

Abstract

In this communication we report the preparation of new ultrahigh modulus tapes from metallocene-based linear polyethylene (LPE) using tensile drawing. Samples have been prepared with a draw ratio in excess of 50 and a room temperature Young's modulus of 103 GPa. The findings represent a natural extension of the previously reported universal relationship between the modulus and the draw ratio. WAXS measurements suggest that the crystal size in the chain direction is as high as 460 Å while SAXS measurements indicate a long period of about 200 Å. This apparent contradiction is resolved by the inter-crystalline bridge model which correlates the modulus with the degree of crystal continuity determined from the longitudinal crystal thickness and the long period. The increase in modulus is attributed to an increase in crystallinity and crystal continuity along the draw direction without any extended chain crystallisation.

Keywords: Ultra-high modulus; Ultra-drawing; Metallocene

1. Introduction

It is well known that tensile deformation of polymers in the solid state increases the stiffness in the deformation direction. There is thus considerable interest in using mechanical deformation to produce polymers with a high degree of molecular alignment and high stiffness [1]. The problem is to establish the conditions required to produce high degrees of molecular orientation.

The factors which determine the preparation of high modulus polymers by tensile drawing have been established by Ward and co-workers [2,3], primarily for linear polyethylene (LPE). A common finding for different polymers was that the Young's modulus is uniquely related to the draw ratio, irrespective of the molecular weight and molecular weight distribution of the polymer. The highest draw ratios which have been reported for polyethylene are for a combination of extrusion and drawing of ultra high molecular weight polyethylene (UHMWPE) by Porter and co-workers [4]. Total draw ratios in the range 200–300 were obtained, giving a Young's modulus of ~220 GPa. For molecular weights in the range up to $M_W \sim 800{,}000$, the maximum draw ratios which have been obtained by tensile drawing are much lower, ~30–40, with a Young's modulus ~70 GPa [5]. Although this is as stiff as aluminium, it is only one quarter of the estimated room temperature crystalline modulus in the chain direction (~285 GPa) [6]. Approaching this ultimate limit more closely is still, therefore, a worthy technological challenge.

Recently, a new generation of metallocene catalysts was invented [7–9]. These catalysts differ from their conventional counterparts in that they have only one active centre and hence the resulting polymer molecules are closely similar. A conventional Ziegler–Natta catalyst, however, has several active centres, each of which produces a different polymer, different both in terms of molecular weight and tacticity where relevant. A metallocene catalyst allows the possibility of preparing polymers with a narrower molecular weight distribution and with any co-monomer units more uniformly distributed throughout the polymer chains.

This work therefore investigates the possibility of producing ultrahigh modulus tapes with enhanced mechanical stiffness by drawing of metallocene based LPE.

2. Experimental

2.1. Sample preparation and characterisation

The materials used in this study are described in Table 1.

* Corresponding author. Tel.: +44-0113-2333808; fax: +44-0113-2333846.

E-mail address: i.m.ward@leeds.ac.uk (I.M. Ward).

0032-3861/01/$ - see front matter
PII: S0032-3861(00)00575-9

Table 1
Material characteristics

Material	M_W	M_W/M_N	Type	Manufacturer
A	154,200	2.69	Metallocene	BP
B	171,700	7.15	Metallocene	Hoechst
C	424,800	5.64	Metallocene	Hoechst
D	149,400	8.69	Conventional	BP

Materials A, B and C are metallocene-based LPE whereas D is a conventional commercial polyethylene (Rigidex HD6007) for comparison purposes.

Oriented samples were prepared from these materials following previous procedures established at Leeds University [3]. Isotropic sheets, 1 mm thick, were prepared by compression moulding at 160°C. Some sheets were quenched into cold water while others were left to cool slowly in the press through the night. Dumbbell-shaped specimens of gauge dimensions 20×5 mm^2 were cut from the sheets and drawn in air at the required drawing temperature at a cross-head speed of 10 cm/min. To determine the draw ratio, samples were marked with ink dots at 1 mm spacing along the gauge length. The positions of these dots, after drawing, were fitted by a fourth order polynomial, the derivative of which gave the draw ratio as a function of position in the sample. The samples on which the experiments were performed were cut from a region of homogeneous draw ratio of at least 10 cm in length.

2.2. Mechanical properties

2.2.1. 10 s creep moduli

The room temperature 10 s creep moduli were measured for a series of drawn specimens of each material. The measurements were used to assess the effectiveness of the drawing and to establish a continuity with the previous measurements made on highly oriented samples prepared from conventional LPE. The measurements were performed using the dead-load creep apparatus, described elsewhere [10]. The strain was measured 10 s after the load application within a strain limit of 0.1%. The modulus was obtained using a linear fit of the resulting strain–stress curve.

2.2.2. Dynamic tensile measurements

The dynamic tensile modulus and loss factor were measured over a range of temperatures using apparatus which has been described in detail elsewhere [11]. The samples, of 5 cm gauge length, were mounted between two clamps inside a temperature controlled chamber. The measurements were performed at a frequency of 3 Hz at 0.05% peak to peak strain and a dead load corresponding to approximately 0.1% static strain.

Table 2
The optimum drawing temperature and the maximum draw ratio achieved for each material

	T_d/°C	λ_{max}	Initial morphology
A	75	39	Slow cooled
B	75	50	Slow cooled
C	110	41	Slow cooled
D	75	40	Slow cooled

2.3. X-Ray measurements

2.3.1. Longitudinal crystallite thickness measurements

WAXS measurements were used to characterise the drawn specimens. In particular, the crystal coherence length (size) along the draw direction was assessed by measuring the sharpness of the (002) reflection. Measurements were performed using a Siemens two circle diffractometer with nickel filtered CuKα radiation. The counting time, chosen to accumulate around 10 thousand counts at the peak maximum, was typically 100 s and the recording interval was 0.02° in 2θ. Values for the average crystal size in the c-axis direction, L_{002}, were obtained from the corrected integral breadth of the (002) reflection using the Scherrer equation as explained elsewhere [12]. The apparatus line shape was determined using a thin annealed nickel foil which contained crystallites large enough to give negligible broadening but small enough to yield a powder pattern.

2.3.2. Long period measurements

SAXS measurements were performed to determine the long period in the drawn specimens. SAXS patterns were obtained using an Anton Paar pinhole small angle camera coupled to a Siemens HI-STAR area detector. Nickel filtered CuKα radiation was used with a sample to detector distance of 42 cm and data were corrected for detector sensitivity and background scattering. Typically, the collection time was 900 s. The long period was obtained from linearly averaged slices parallel to the orientation direction through the central part of the pattern.

2.4. Differential scanning calorimetry

A Perkin Elmer DSC-7, operating at a heating rate of 10°C min^{-1}, was used to measure crystallinity. The DSC was calibrated using a standard indium sample. Heats of fusion were determined from the area under the sample melting curve between 120 and 145°C and the crystallinity, χ, was found using a value of 293 J/g [13] for the heat of fusion of a perfect polyethylene crystal.

3. Results

Preliminary investigations were performed to determine the optimum drawing temperature for each sample. This is the temperature which gives maximum modulus, rather than maximum draw ratio since the latter can be achieved by flow at high temperatures, rather than molecular alignment. Table 2 gives the optimum drawing temperature, T_d, and the maximum draw ratio achieved for each sample.

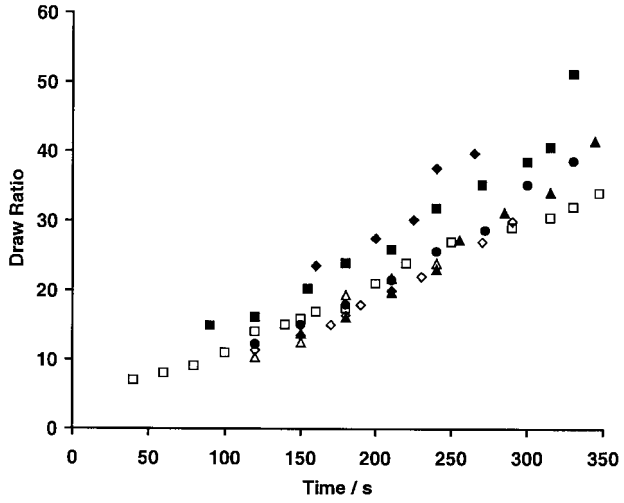

Fig. 1. The maximum relaxed draw ratio as a function of drawing time. Open symbols quenched, solid symbols slow cooled: ○ A; □ B; △ C, ◇ D.

The effect of the initial morphology on the drawing behaviour and the maximum drawability was studied using both slow cooled and quenched sheets of materials B, C and D but only slow cooled sheets of material A. Fig. 1 shows the maximum draw ratio as a function of drawing time for the different materials and morphologies. The upper limit on the time scale for samples A, C and D was imposed by a sample failure. Sample B did not fail, however, but drew until no further extension could be achieved in the temperature chamber.

Fig. 2 shows the 10 s Young's moduli along the draw direction as a function of the draw ratio. It can be seen that material B could be drawn to remarkably high draw ratios, around 50:1, which is the highest value recorded for solid phase tensile deformation in a single stage. The drawing was accompanied by a considerable enhancement in the room temperature Young's modulus where the high value of 103 ± 4 GPa was achieved. The other metallocene-based materials, A and C, could be drawn to reasonably high draw ratios with corresponding room temperature Young's moduli but their behaviour was comparable with that of the conventional LPE (material D).

In the light of these results, further investigations concentrated upon comparisons of material B with the conventional material D. Three samples were chosen: two of material B with draw ratios of 30 and 50, (B-30 and B-50, respectively) and a third sample of material D with a draw ratio of 30, (D-30). Sample B-50 represents the new ultra-high modulus samples prepared from the metallocene-based LPE while B-30 and D-30 allow comparison of the two different materials at the same draw ratio.

The load–elongation curves and dynamic mechanical behaviour of these samples were determined and information about their microstructure was obtained from WAXS, SAXS and DSC measurements.

3.1. Load–elongation curves

Fig. 3 shows the load–elongation curves for samples B and D (of the same initial dimensions) during drawing at 75°C. Both samples show a sharp yield point, corresponding to the onset of necking but the drawing stress was always greater for sample B. Sample D broke at a true stress of 290 MPa while sample B sustained a true stress of 450 MPa at the end of drawing period without breaking.

3.2. Dynamic tensile behaviour

The dynamic tensile moduli of the three samples were measured in the temperature range −150 to 25°C. Each specimen was held under a slight tension at 25°C for at least 30 min and then the temperature was dropped to −150°C in 10°C intervals. The temperature dependence of storage modulus and tan δ is shown in Fig. 4. It can be seen that the data for the two draw ratio 30 samples are similar

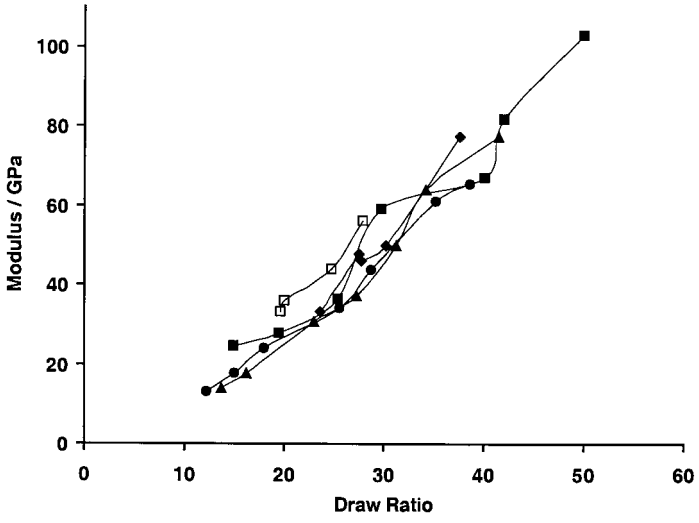

Fig. 2. The 10 s Young's modulus as a function of draw ratio. Key as Fig. 1.

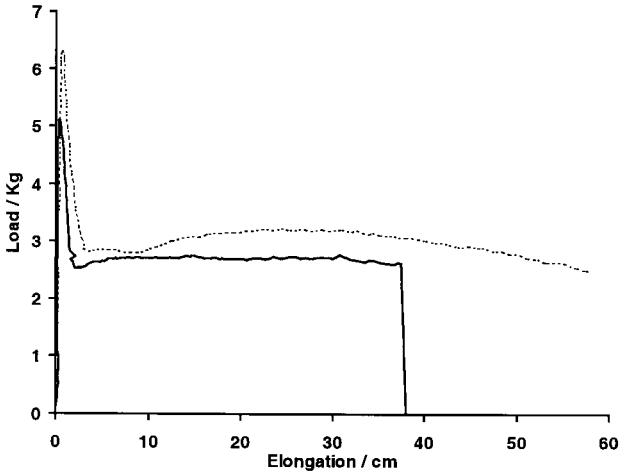

Fig. 3. The load–extension curves for samples of B and D during drawing at 75°C. Broken line B, solid line D.

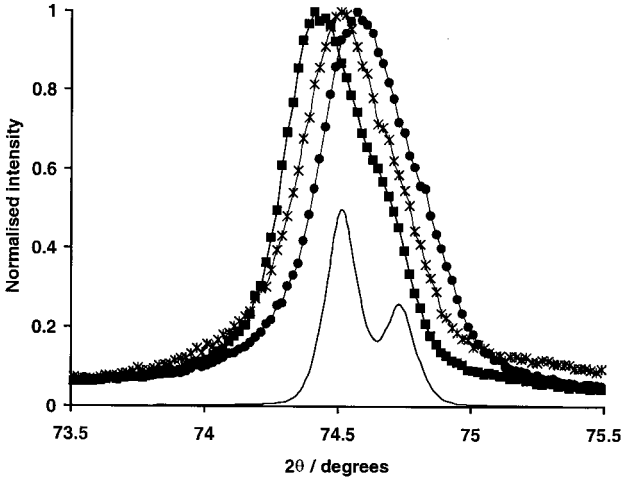

Fig. 5. The WAXS 2θ scans through the 002 reflection of samples D-30, B-30 and B-50. Key as Fig. 4 plus solid curve for the apparatus profile.

but that sample B-50 exhibits an enhanced modulus over the complete temperature range studied, a value of 150 GPa being recorded for this sample at −150°C.

3.3. WAXS measurements

The 2θ breadth of the 002 reflection of these highly oriented samples provides a measure of the crystal size in the direction of the chain axis. Fig. 5 shows the experimental (002) reflection profiles for the three samples, together with the instrumental broadening profile. The main peak arises from the $CuK\alpha_1$ line while the slight bump on the right hand side of each experimental peak arises from the $K\alpha_2$ line which is well resolved in the instrumental profile. The influence of this $K\alpha_2$ peak is more obvious for B-50 curve which immediately suggests that this sample has a greater *c*-axis correlation length since it provides the more highly resolved line shape. Quantitative analysis yields the longitudinal crystalline thicknesses, L_{002}, listed in Table 3.

The difference between the peak positions for samples B-50 and D-30 of 0.16° in 2θ may not be significant though repeated scans of remounted samples gave a scatter of only about 0.05° in 2θ. The higher drawing stress for sample B could possible be reflected in a greater lattice strain of the order of 0.2% but structural features which could maintain this strain are not readily identifiable.

3.4. SAXS measurements

SAXS patterns for the three samples are shown in Fig. 6. The main feature of these patterns is the intense equatorial streak. This streak, which arises from elongated microvoids [14], is much more pronounced for the B-50 sample as might be expected from its higher draw ratio. A weak meridional 2-point pattern is also apparent, however, which was

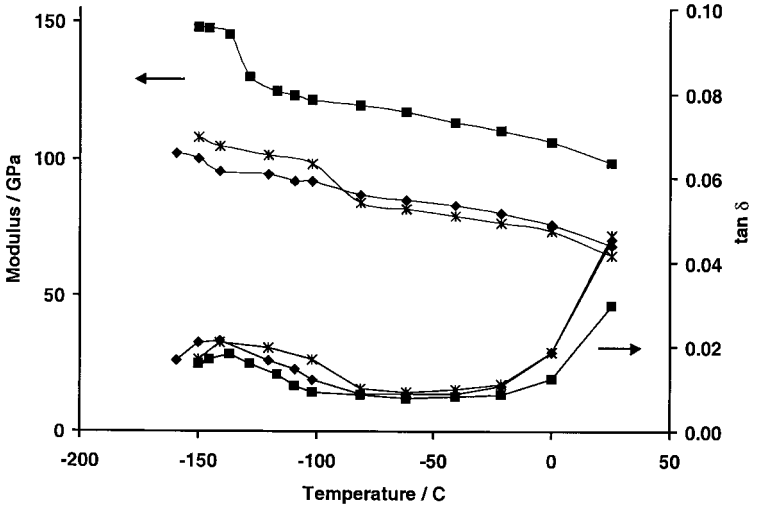

Fig. 4. The 3 Hz dynamic tensile modulus and tan δ as a function of temperature for samples D-30, B-30 and B-50. ◆ D-30, ∗ B-30, ■ B-50.

Table 3
The results of structural characterisation of samples D-30, B-30 and B-50

	D-30	B-30	B-50
L_{002} (Å)	366 ± 8	382 ± 11	460 ± 18
L (Å)	197 ± 10	205 ± 12	201 ± 14
(χ (%)	79	79	86
p	0.30	0.30	0.39
Ψ	0.64	0.66	0.70

used to determine the lamellar spacing, L, of the samples reported in Table 3.

It was initially feared that the intensity of this peak was too low to allow accurate determination of the periodicity. Previous studies have shown, however, that the long spacing of a deformed polymer depends primarily on the temperature of the deformation and not on the draw ratio [15]. The long spacings for low draw ratio samples of materials B and D, drawn at the same temperatures as the high draw ratio samples, were therefore measured. Samples with a draw ratio about 9:1 yielded values of 195 ± 7 Å and 202 ± 6 Å for materials B and D, respectively. These data are comparable with those found for the higher draw ratio samples and hence the higher draw ratio figures can be used with more confidence.

3.5. DSC measurements

The melting curves for the three samples are shown in Fig. 7. It can be seen that the traces are similar in shape, although the area per unit mass under the peak for B-50 is larger than that of B-30 and D-30, which show comparable areas. Furthermore, the peak position for sample B-50 is higher than that for the B-30 and D-30 samples. The derived crystallinities, χ, are listed in Table 3.

3.6. Crystal continuity analysis

Gibson et al. have proposed a structural model for highly oriented polymers in order to quantify the improvement of the stiffness with draw ratio [16]. According to this model,

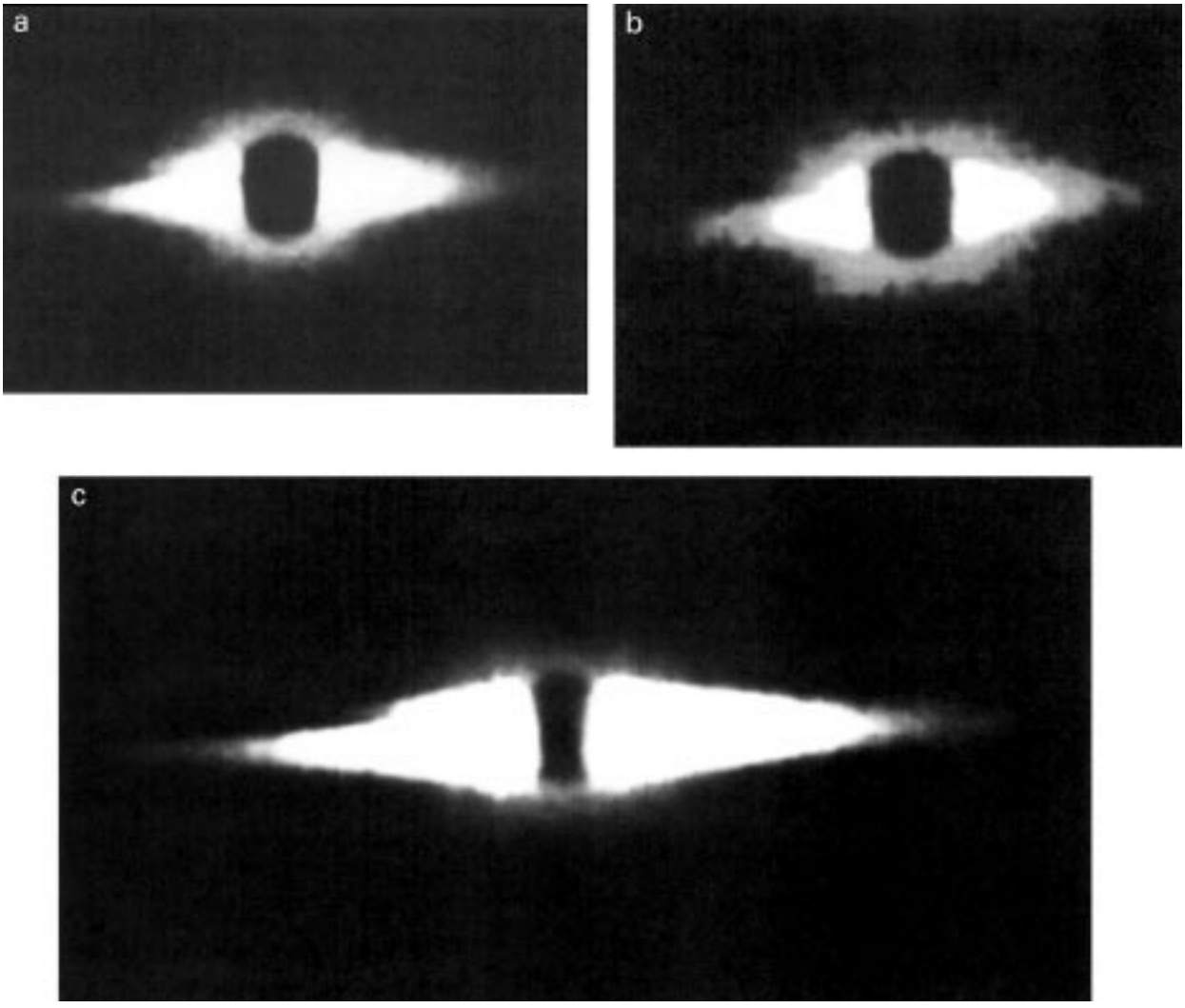

Fig. 6. The SAXS patterns of: (a) D-30; (b) B-30 and (c) B-50.

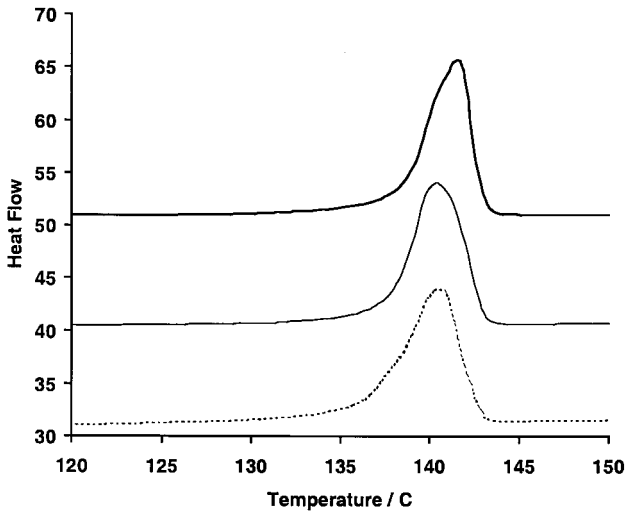

Fig. 7. The DSC curves for samples D-30, B-30 and B-50 samples at heating rate of 10°C/min. Broken line D-30, light solid line B-30 and heavy solid line B-50 (curves displaced vertically for clarity).

the structure of these highly oriented polymers may be modelled as oriented stacks of lamellae which are linked by inter-crystalline bridges. These bridges, which are assumed to be randomly distributed, provide a degree of crystalline continuity which increases the mean longitudinal crystal thickness and allows it to be greater than the lamellar periodicity. The parameter p, which defines the probability of a crystalline sequence traversing the intercrystalline region to link two adjacent lamellae, can be calculated from:

$$p = \frac{L_{002} - L}{L_{002} + L} \tag{1}$$

The inter-crystalline bridge model then predicts that:

$$\frac{E'}{E_c} = \Psi\chi p(2 - p) \tag{2}$$

where E_c is the crystal modulus in the chain direction and Ψ is a "shear lag" factor which allows for the ineffective length of the ends of the bridges where the tensile stress decays to zero. The correlation with the Young's modulus E' was originally made at a temperature of −50°C rather than room temperature since the latter data are sensitive to changes in the α-relaxation brought about by drawing. At −50°C the material is between the α and γ relaxations and viscoelastic effects are minimised.

The model is used here to relate the mechanical stiffness to the structure of the D-30, B-30 and B-50 samples. From the dynamic behaviour shown in Fig. 4 it can be seen that the moduli show a plateau region between the α and γ relaxations, around −55°C. Therefore, the −55°C moduli were taken to represent the non-viscoelastic stiffness of these samples. Table 3 shows the results obtained by fitting the experimental data to Eq. 2 with Ψ as an adjustable parameter and assuming $E_c = 314$ GPa [6] (the 200 K value, being the nearest to −55°C).

4. Discussion

The most outstanding result of this work was the preparation of new ultrahigh modulus samples. These samples showed a very high draw ratio (~50) and room temperature Young's modulus (~103 GPa). This represents a natural extension of the previous work on highly oriented polymers carried out by the Leeds group [1].

The effect of the drawing conditions on the drawing behaviour of the metallocene-based LPE is similar to that found for conventional LPE. The optimum draw temperature was correlated with the molecular weight such that for high molecular weight samples it was necessary to increase the draw temperature to obtain the most effective drawing behaviour.

The initial thermal treatment had much more effect on the drawing behaviour for the sample with intermediate molecular weight (sample B). However, this effect was not pronounced for high molecular weight sample (sample C). Generally speaking, slow cooled sheets showed higher draw ratios than those prepared by rapid quenching. Furthermore, the rate of deformation in the necked regions was slightly higher in the slow cooled sheets than in the quenched sheets.

This difference has been related to the different structures evolved by the two thermal treatments [17]. In quenched sheets, crystallisation occurs at high supercooling, which means high internal viscosity of the polymer and so a complex spherulitic geometry with high amount of twisting and branching is produced. In slow cooled sheets, crystallisation occurs at low supercooling and hence low viscosity, which results in more uniform lamellar structure with less branching. Consequently, the more regular structure of the slow cooled sheets deforms more easily than that of quenched sheets.

The modulus-draw ratio curves for these samples showed a good correlation between the Young's modulus and the draw ratio. These results demonstrate that the modulus is determined primarily by the macroscopic deformation of the polymer irrespective of its molecular weight, molecular weight distribution or its initial morphology. This is consistent with the previously reported universal relationship between modulus and draw ratio but extends it to a higher range of moduli and draw ratios.

The drawing curves of Fig. 3 show that the drawing stress of sample B was higher than that of the conventional LPE sample. This difference continues through the whole drawing process where comparison can be made. The difference suggests that the initial structure of sample B allows a more homogeneous stress transfer through the specimen thus reducing stress concentration and necessitating higher bulk stresses to achieve a given deformation.

The most outstanding feature of the dynamic tensile

measurements is the high modulus of B-50 at −150°C (~150 GPa). The intensity of the γ-relaxation for B-50 sample is somewhat lower than those of the B-30 and D-30 samples. The γ-relaxation is generally considered to be comprised of components from both the amorphous and crystalline phases [18]. The amorphous phase contribution, however, is more dominant. Therefore, the lower intensity of the γ-relaxation for B-50 sample can be explained in terms of its higher crystallinity and also crystalline continuity. The crystalline continuity constrains what is left from the amorphous phase and thus the amorphous contribution is further decreased which results in a lower magnitude of the γ-relaxation and higher modulus above the γ-relaxation.

The α-relaxation is usually related to the crystalline phase. The magnitude of this relaxation was found to be inversely proportional to the lamellar thickness [19]. Since high crystalline continuity has been developed in B-50 sample, this could explains the apparent lower magnitude of α-relaxation for B-50 sample. A shift to higher temperatures, which might also be expected, cannot be ruled out by these data, however.

The longitudinal crystalline size measurements yield values as large as 460 Å for the high-modulus sample B-50. The corresponding values for samples B-30 and D-30 were only 382 and 366 Å, respectively, which indicates an increase in the crystal continuity in the chain direction with increasing the macroscopic deformation. This is not to be taken as evidence for the production of chain extended crystals in these new high modulus samples, however, since the average longitudinal crystal size are still much lower than those typically found for extended chain crystals (~1000 Å) [20].

The long spacings deduced from the SAXS measurements show no significant change with draw ratio. This is in agreement with previous work performed on conventional LPE [21]. The patterns show that a periodic density fluctuation with a period in the deformation direction of approximately 200 Å for B and D specimens still exist even after the very large macroscopic deformations imposed on the B sample.

The DSC measurements imply that crystallinity as high as 86% has been developed in the new high-modulus samples (B-50) which melts at the high melting point of 141.5°C. Such a high value has been observed in pressure crystallised isotropic samples, which show extended chain crystals. The possibility of existence of such extended chains in B-50 can be excluded for two reasons, however: the WAXS crystalline thickness measurements do not suggest this possibility (though they cannot rule out a small fraction of highly extended material); and if there was a fraction of the crystalline material in extended chain form, then multiple peaks should be observed in the melting curve. Multiple peaks are not observed, however. The elevated melting point for the B-50 sample (which is still 139.8°C at the lower heating rate of 1°C/min) can be explained through the superheating effect as proposed for conventional highly oriented polymers [22]. This effect can be understood in terms of the increase in the crystalline continuity which results in increasing constraints on the non-crystalline chains as the draw ratio increased. Hence, configurational restrictions during the melting process lead to very small entropy variations between the solid and molten state. This gives rise to an apparent melting temperature higher than the equilibrium thermodynamic melting temperature of the crystals.

The new ultrahigh modulus samples fit within the previously proposed crystalline bridge model. The parameter p relates to the crystalline continuity within the oriented polymer. It varies from zero for a specimen with a perfect series arrangement of phases up to unity for a perfect parallel arrangement. The structural studies yield a p value for the B-50 sample which is higher than that of the B-30 and D-30 samples which showed comparable values. This indicates the higher crystalline continuity achieved by deforming sample B to such high draw ratio is a major reason for its increased modulus. A secondary effect of the increased continuity is a reduction in the influence of shear lag (i.e. a shear lag factor closer to unity) arising from the increased aspect ratio of the stiffening elements.

The natural question to be asked here is why does sample B shows such high drawability? To help answer this question, the morphology of isotropic and drawn specimens of the different materials was studied by transmission and scanning electron microscopy [23]. It was found that all samples eventually develop a characteristic longitudinal periodic structure with a period of about 5–15 μm on drawing. Once this structure has been developed, the specimens fail under increased deformation and higher draw ratios are not attainable. For reasons not obvious at the moment, sample B shows a delay in developing this structure and high draw ratios are obtained. More extensive studies are currently being undertaken to quantify the factors which affect the development of such structure.

5. Conclusions

In this study, the possibilities of preparing new ultrahigh modulus samples from a new generation of metallocene-based LPE, were explored. New ultra-high modulus tapes of draw ratio ~50 and room temperature Young's modulus ~103 GPa were prepared. The dynamic tensile behaviour showed that these ultra-high modulus tapes have a modulus of 150 GPa at −150°C. This is due to their high crystallinity and a high degree of crystalline continuity as revealed by the structural measurements. The crystalline bridge model was shown to be adequate to interpret the mechanical behaviour of these new ultrahigh modulus tapes and reconciled the high values of the crystalline thicknesses shown by these samples with their much smaller long periods.

In comparison with conventional LPE, apart from the capability to be drawn to higher draw ratios, there was not that much of difference. The only noticeable difference was

in their load–elongation curves. These new samples showed a higher drawing stress which may be taken as an indication of a more uniform stress distribution which delays failure and allows high deformations to be achieved.

Electron microscopy studies of drawn samples show that all samples develop a characteristic longitudinal periodic structure before failing under subsequent deformation. Sample B showed a delayed development of such a structure. The reasons for this delay are now under investigation.

Acknowledgements

We would like to thank The Arab-British Charitable Foundation for their financial support of M. Al-Hussein.

References

[1] Ciferri A, Ward IM, editors. Ultra-high modulus polymers. London: Applied Science Publishers, 1977.
[2] Andrews JM, Ward IM. J Mater Sci 1970;5:411.
[3] Capaccio G, Compton TA, Ward IM. J Polym Sci (Phys) 1976;14:1641.
[4] Zachariades AE, Kanamoto T. In: Zachariades AE, Porter RS, editors. High modulus polymers: approaches to design and development. New York: Marcel Dekker, 1988 (chap. 10).
[5] Ward IM. Adv Polym Sci 1985;70:1.
[6] Lacks DJ, Rutledge GC. J Phys Chem 1994;98:1222.
[7] Thayer AM. Chem Engng 1995;73:15.
[8] Eckstut M, Kuhlke W, Peterson F. Chem Engng 1996;103:92.
[9] Hiarston DW. Chem Engng 1995;102:59.
[10] Gupta VB, Ward IM. J Macromol Sci (Physics) 1967;B1:373.
[11] Troughton MH, Davies GR, Ward IM. Polymer 1981;30:58.
[12] Al-Hussein M, Davies GR, Ward IM. J Polym Sci, Part B: Polym Phys 2000;38:755.
[13] Wunderlich B. Macromolecular physics, vol. 1. New York: Academic Press, 1973.
[14] Grubb DT, Prasad K. Macromolecules 1992;25:4575.
[15] Peterlin A, Corneliussen R. J Polym Sci, A-2 1968;6:1273.
[16] Gibson AG, Davies GR, Ward IM. Polymer 1978;19:683.
[17] Capaccio G, Ward IM. Polymer 1975;16:239.
[18] Boyd RH. Polymer 1985;26:323.
[19] Sinnot KM. J Appl Phys 1966;37:3385.
[20] Clements J. Lattice modulus and crystal thickness measurements on ultra-high modulus linear polymers. PhD thesis. University of Leeds, 1978.
[21] Clements J, Ward IM. Polymer 1983;24:27.
[22] Clements J, Capaccio G, Ward IM. J Polym Sci, Phys 1979;7:693.
[23] Amornsakchai T, Olley RH, Basset DC, Al-Hussein M, Unwin AP, Ward IM. Polymer 2000 (in press).